

Indicator Dyes and Catalytic Nanoparticles for Irreversible Visual Hydrogen Sensing

Michael E Smith, Angela L Stastny, John A Lynch, Zhao Yu, Peng Zhang, and William R. Heineman

Anal. Chem., **Just Accepted Manuscript** • DOI: 10.1021/acs.analchem.0c01769 • Publication Date (Web): 06 Jul 2020

Downloaded from pubs.acs.org on July 13, 2020

Just Accepted

“Just Accepted” manuscripts have been peer-reviewed and accepted for publication. They are posted online prior to technical editing, formatting for publication and author proofing. The American Chemical Society provides “Just Accepted” as a service to the research community to expedite the dissemination of scientific material as soon as possible after acceptance. “Just Accepted” manuscripts appear in full in PDF format accompanied by an HTML abstract. “Just Accepted” manuscripts have been fully peer reviewed, but should not be considered the official version of record. They are citable by the Digital Object Identifier (DOI®). “Just Accepted” is an optional service offered to authors. Therefore, the “Just Accepted” Web site may not include all articles that will be published in the journal. After a manuscript is technically edited and formatted, it will be removed from the “Just Accepted” Web site and published as an ASAP article. Note that technical editing may introduce minor changes to the manuscript text and/or graphics which could affect content, and all legal disclaimers and ethical guidelines that apply to the journal pertain. ACS cannot be held responsible for errors or consequences arising from the use of information contained in these “Just Accepted” manuscripts.

Indicator Dyes and Catalytic Nanoparticles for Irreversible Visual Hydrogen Sensing

Michael E. Smith, Angela L. Stastny, John A. Lynch, Zhao Yu, Peng Zhang*, William R. Heineman*

University of Cincinnati, Department of Chemistry, Cincinnati, OH 45221-0172 USA

ABSTRACT: Using ultraviolet-visible (UV-Vis) absorption spectroscopy, we have tested the reactivity of various indicator molecules combined with catalytic bimetallic gold-palladium nanoparticles (Au-Pd NPs) in solution for irreversible, and visual response to H₂ with the aim to develop the most suitable indicator/Au-Pd NP system into a thin, wearable, and visual H₂ sensor for non-invasive monitoring of *in vivo* Mg-implant biodegradation in research and clinical settings with fast response time. The indicators studied were bromothymol blue, methyl red, and resazurin, and the reactions of each system with H₂ in the presence of Au-Pd NPs caused visual and irreversible color changes that were concluded to proceed via redox processes. The Resazurin/Au-Pd NP system was deemed best suited for our research objectives because (1) this system had the fastest color change response to H₂ at levels relevant to *in vivo* Mg-implant biodegradation compared to the other indicator/Au-Pd NP systems tested, (2) the observed redox chemistry with H₂ followed well-understood reaction pathways reported in the literature, and (3) the redox products were non-toxic and appropriate for medical applications. Studying the effects of the concentrations of H₂, Au-Pd NPs, and resazurin on the color change response time within the Resazurin/Au-Pd NP system revealed that the H₂ sensing elements can be optimized to achieve a faster or slower color change with H₂ by varying the relative amounts of resazurin and Au-Pd NPs in solution. The results from this study are significant for future optical H₂ sensor design.

Magnesium (Mg) and its alloys have the capability of outperforming traditionally used materials for orthopedic applications such as bone repair because they can act as load-bearing implants that safely biodegrade when no longer needed.¹⁻¹¹ We have previously shown that an appreciable fraction of the hydrogen gas (H₂) liberated as a corrosion product from Mg-implant biodegradation can be detected transdermally and non-invasively at levels ranging from ~30 to ~700 μM by placing electrochemical or visual H₂ sensors on mouse skin directly above implants as they biodegraded *in vivo*.^{2,5,6,12} These non-invasive H₂ sensing methods are considered to be fast, reliable, and accurate representations of the extent of *in vivo* Mg-implant biodegradation since the measured H₂ levels correlated nicely with the biodegradation rates measured via the highly accurate mass loss method of explanted implants.^{2,5} These significant discoveries opened the door to using H₂ sensing as a platform for monitoring the *in vivo* biodegradation of Mg-implants by a simple, non-invasive procedure without exposure to X-rays. Furthermore, this sensing platform enables *in vivo* biodegradation to be measured in real-time. These features are desirable in medical research settings in which new biodegradable materials and devices are developed and in clinical settings for the routine evaluation of patients with Mg-implants. However, the sensors used in the aforementioned studies are limited for monitoring H₂ in such settings. For example, the electrochemical H₂ sensor offers remarkable sensitivity, yet the sensor itself and the associated instrumentation are costly, complex, and require a reasonable skill level for proper use. This sensor also requires regular calibration and tedious multiple measurements if mapping of H₂ levels over an area above an implant is desired since the sensor surface is ~50 μm in diameter. The visual H₂ sensor of ~10 μm thickness and ~1 cm² surface area afforded detailed mapping of

H₂ levels above implants, which is a very useful tool for monitoring larger implants such as plates, and the H₂ detection could be made easily using a cell phone.^{5,12} However, the exposure times required to induce detectable color changes were on the order of hours, which limit its practical use. To circumvent these problems, the objective of this research was to test the reactivity of various indicator molecules combined with catalytic bimetallic gold-palladium nanoparticles (Au-Pd NPs) in solution for fast, irreversible, and visual response to H₂ with the aim to later develop the most suitable indicator/Au-Pd NP system into a thin, wearable, and optical H₂ sensing device for non-invasive monitoring of *in vivo* Mg-implant biodegradation in medical research and clinical settings with fast response time.

Nanoparticles (NPs) such as those of platinum (Pt)¹³⁻¹⁷, palladium (Pd)^{5,11,18-20}, and Au-Pd²¹⁻²⁵ have attracted considerable interest for use in a variety of H₂ sensing platforms and applications due to their unique catalytic abilities. Our basis for choosing Au-Pd NPs for our research objectives stems from reports describing how alloys containing Au and Pd are particularly advantageous for H₂ sensing by exhibiting enhanced H₂ adsorption and solubility.^{26,27} With respect to signal transduction for H₂ sensing, catalytic NPs have been combined with different indicators for the development of optical H₂ sensors in which the sensing mechanism relies on the dissociation of H₂ at the NP surface to form highly reactive hydrogen atoms that subsequently undergo a redox reaction with an indicator to cause a visual color change.^{5,13} For example, Seo *et al.*¹³ used a reagent containing methylene blue and Pt NPs to quantify the amount of H₂ dissolved in water as the reagent underwent a blue to colorless transition upon reaction with H₂. Although this simple method was shown to be as effective as an electrochemical sensor for H₂ quantification,¹³ the use of methylene blue as a H₂ sensing molecule is

disadvantageous for certain applications because the reduction of methylene blue and subsequent color change is known to be reversible in the presence of oxygen (O₂).²⁸ Regarding our goal of future optical H₂ sensor development for monitoring Mg-implant biodegradation *in vivo*, the sensing mechanism should ideally be an irreversible process such that the sensor color change resulting from redox reactions between hydrogen atoms, formed at the NP catalyst surface, and indicator molecules cannot be reverted back to the original sensor color by O₂. An optical H₂ sensor with irreversible capabilities would likely achieve the lower limits of detection needed for medical applications since O₂ would not affect the overall color change response time of the sensor. From a practical perspective, our development of an optical H₂ sensor should also exhibit a color change response on the order of ~10 minutes. Therefore, the primary goal of this work was to investigate various indicators that could undergo irreversible color changes upon reaction with H₂ at levels relevant to *in vivo* Mg-implant biodegradation (e.g. ~30 to ~700 μM) in the presence of Au-Pd NP catalysts, and to identify the most suitable indicator/Au-Pd NP system for future optical H₂ sensor development by comparing the color change response time of each system.

The specific indicators investigated in this study were those shown in Figure 1 and included bromothymol blue, methyl red, and resazurin. Bromothymol blue (Figure 1A) is a well-known acid/base indicator that exhibits a blue to yellow color change upon protonation.²⁹ Methyl red (Figure 1B) is another well-known acid/base indicator that has yellow and red colors in the deprotonated and protonated forms, respectively.³⁰ Due to the reported electrochemical reduction pathways in the literature for these molecules,^{31–33} it was hypothesized that bromothymol blue and methyl red could undergo rapid, and irreversible reduction reactions with H₂ in the presence of Au-Pd NP catalysts that would result in visual color changes through a similar mechanism described by Seo *et al.*¹³ for the methylene blue/Pt NP system. Resazurin (Figure 1C), a common redox indicator that exhibits a blue color at neutral pH, can undergo an irreversible reduction to lose water to form a pink-colored, and highly fluorescent resorufin product.^{34–38} A subsequent reduction of resorufin to the colorless dihydroresorufin can occur, but the process is reversible in the presence of O₂.³⁵ Despite reversibility of this subsequent reaction, resazurin was hypothesized to be a good candidate for our research objectives since the initial irreversible reduction that forms the highly luminescent resorufin product would likely be the only color transition observed at low levels of H₂ exposure, and this product could serve nicely as the analytical signal. Furthermore, previous work has shown that resazurin can be converted to resorufin upon reaction with H₂ in the presence of Pt NP catalysts.³⁹

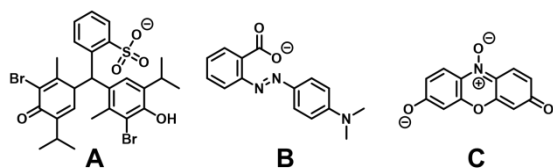


Figure 1. Anions of the sodium salts of (A) bromothymol blue, (B) methyl red, and (C) resazurin.

In this work, we tested the reactivity of H₂ with bromothymol blue, methyl red, and resazurin indicators combined with Au-Pd NP catalysts by preparing buffered solutions (pH~7.5) and exposing each to H₂ at a known flow rate and concentration while ultraviolet-visible (UV-Vis) absorption spectra were monitored over time. The indicator/Au-Pd NP system most suitable for our target application for future optical H₂ sensor development was identified by comparing the changes in the characteristic UV-Vis absorption maxima of each indicator/Au-Pd NP system as a function of H₂ exposure time. The most suitable indicator/Au-Pd NP system was further studied via UV-Vis spectroscopy to examine the effects of varying the concentrations of H₂, Au-Pd NPs, and indicator on the color change response time.

EXPERIMENTAL SECTION

Chemicals, Materials, and Instrumentation. All chemicals and materials were used as received. Resazurin sodium salt (C₁₂H₆N₂NaO₄, >85.0% by HPLC) was purchased from TCI America Inc. Sodium salts of methyl red (C₁₅H₁₄N₃NaO₂) and bromothymol blue (C₂₇H₂₇Br₂NaO₅S) were acquired from ACROS Organics (USA). Gold (III) chloride trihydrate (HAuCl₄·3H₂O, ≥ 99.9% trace metal basis), and potassium hexachloropalladate (IV) (K₂PdCl₆, 99%) were purchased from Sigma-Aldrich (MO). Trisodium citrate dihydrate (Na₃C₆H₅O₇·2H₂O), phosphate buffered saline (PBS, 10X solution, pH 7.4), and a 3-way valve of polytetrafluoroethylene (PTFE) were obtained from Fisher Scientific (NJ). Hydriion pH paper (0–13 range) was obtained from Grainger (IL). All aqueous solutions were prepared using de-ionized water (≥ 18 MΩ·cm, referred to as DI water herein). Ultra-high purity grades of H₂ and N₂ gases were obtained from Wright Brothers Inc. (OH). A gas proportioning rotameter (#GMR2-010343) equipped with two flow tubes (FL-2GP-61C-61C) was purchased from Omega Engineering (CT). A rotameter with a single flow tube (#FP 1/8-038-G-6) was acquired from Lab-Crest, Fisher & Porter Co. (PA). Tygon tubing (1/4" ID, 1/2" OD) was purchased from McMaster-Carr (OH). Hypodermic needles (305120-23G) were acquired from BD Co. (NJ). Stainless-steel tubing (1/8" OD) was purchased from Supelco (PA). An amperometric H₂ sensor (H₂-NP-705273) and multimeter were obtained from Unisense (Denmark). A DryCal DC-Lite flow calibrator was acquired from Brandt Instruments, Inc. (LA). Microcentrifuge tubes were purchased from Avant (MO). NPs were centrifuged using a Sorvall, Legend Micro 21 (MA). UV-Vis spectra of all samples were collected using a USB4000-UV-VIS spectrophotometer (Ocean Optics, FL) by loading samples in a 1 cm × 1 cm quartz cuvette. For all time-based UV-Vis spectra, data shown at t ≥ 0 seconds correspond to gas being delivered into samples while data at t < 0 seconds correspond to no gas being delivered into samples. Transmission electron microscopy (TEM) measurements of NP samples were performed on a Biotwin 12 TEM (FEI) by depositing a drop of solution on a formvar-covered, carbon-coated copper grid (Electron Microscopy Sciences, PA) and letting the solvent dry at room temperature. Size distributions, average hydrodynamic diameters (\bar{d}), and zeta potentials (ζ) of NP samples were measured using dynamic light scattering (DLS) instrumentation (Microtrac, USA).

Synthesis of Au-Pd Bimetallic Nanoparticle Master Solution. Au-Pd NPs were synthesized by the co-reduction of

[AuCl₄]⁻ and [PdCl₆]²⁻ ions via trisodium citrate as described previously with slight modifications.⁴⁰ A batch of Au-Pd NP solution was prepared by gently boiling and vigorously stirring a solution containing 312 μL of 20 mM HAuCl₄·3H₂O, and 312 μL of 20 mM K₂PdCl₆ at a total volume of 50.00 mL in DI water. Three mL of 2% (m/V) trisodium citrate was added quickly, and the solution was left to boil under vigorous stirring for 15 minutes. The solution was then cooled to room temperature before being stored in the dark at ~4°C until further use. A total of five batches of Au-Pd NPs were prepared and combined in the following way to make a highly concentrated Au-Pd NP master solution. Firstly, the contents of five batches were transferred to one borosilicate Erlenmeyer flask and boiled, uncovered, under vigorous stirring until the solvent level reached ~25 mL. This solution was left to cool to room temperature and the contents were transferred into several microcentrifuge tubes and centrifuged at 14,000 rpm for 20 minutes. The supernatants were discarded to waste while the pellets of Au-Pd NPs remained in the bottom of each tube. All pellets were sonicated, creating highly concentrated micro volumes of Au-Pd NPs, and combined into a borosilicate glass container thereby creating a highly concentrated solution of Au-Pd NPs with a volume of ~5.00 mL in DI water. This solution will be referred to as the Au-Pd NP master solution herein.

Gas Flow Setups and Determining the Concentration and Flow Rate of H₂ Delivered to Samples. The general gas flow setup for various experiments is depicted in Figure S1. Using appropriate fittings and stainless-steel tubing, H₂ and N₂ gas tanks were fitted with regulators then connected to the inlets of a gas proportioning rotameter (GPR) containing two separate flow tubes for H₂ and N₂ (labeled “GPR-H₂” and “GPR-N₂” in Figure S1). Varying the flow rates of H₂ and N₂ in the GPR flow tubes permitted the ability to make a sample mixture of H₂/N₂ gas at a particular volume to volume ratio (v/v) based on the respective GPR flow tube scale readings. The outlet of the gas proportioning rotameter was connected to a rotameter equipped with a single flow tube to allow controlled flow of sample gas. The outlet of this flow tube was then connected to a 3-way valve via stainless-steel and Tygon tubings. Lastly, stainless-steel tubing was connected to the remaining outlets of the 3-way valve to allow directional flow of sample gas to vent or to an experiment at a controlled rate. Flow rate data of N₂ and H₂ gases from the GPR flow tubes at various scale readings were provided by Omega Engineering (Table S1), and plots of gas flow rate (mL/min) vs. rotameter scale reading (mm) were made for each gas and fit to quadratic equations (Figure S2). To create a H₂/N₂ gas mixture with a desired volume percentage of H₂ (%V_{H₂,theoretical}), a reasonable flow rate of H₂ at the GPR flow tube (*GPR:H₂ flow rate*) was chosen. Equation S1 was then used to calculate the necessary flow rate of N₂ at the GPR flow tube (*GPR:N₂ flow rate*) that would achieve the desired value of %V_{H₂,theoretical}. To determine the precise GPR flow tube scale readings for H₂ and N₂ that would achieve the desired %V_{H₂,theoretical}, the flow rates (y-values) for the respective gases were plugged into the corresponding quadratic equations from Figure S2 to solve for the scale readings (x-values).

To deliver gas at a known rate to an experiment from the single flow tube rotameter, this flow tube needed to be calibrated. This was accomplished using a DryCal DC-Lite

flow calibrator for pure N₂ and measuring the flow rate at various scale readings. It was deemed unsafe to measure H₂ flow in either pure or mixed forms using the DryCal DC-Lite flow calibrator due to potential sparking hazards. Thus, flow rates of pure H₂ coming from the single flow tube rotameter at various scale readings were calculated theoretically using Equation S2 where *R*, *Q*, and *ρ* represent the rotameter scale reading (mm), volumetric flow rate (mL/min), and gas density (g/L).⁴¹ The gas densities of pure N₂ and H₂ used were 1.25 g/L and 0.09 g/L, respectively, and were determined using the ideal gas law at standard temperature and pressure. When comparing flow rates for two gases at the same rotameter scale reading, (i.e., where *R*₁ = *R*₂), Equation S2 reduces to Equation S3.⁴¹ The rotameter calibration for N₂ could therefore be applied to pure H₂ using Equation S3.⁴¹ The measured flow rates for pure N₂ and calculated flow rates of pure H₂ at various scale readings are summarized in Table S2.

For flow rate determinations of H₂/N₂ gas mixtures, it was necessary to measure the concentration of H₂ within the mixture using an amperometric H₂ sensor to calculate theoretical gas densities. To do so, an amperometric H₂ sensor was calibrated as described previously.^{1,5,6} The sensor was connected to a multimeter and polarized at +1000 mV for at least one hour before use. Pure H₂ was delivered into ~20 mL of DI water at 257 mL/min for 30 minutes to form a 100% saturated H₂ solution constituting an 800 μM concentration at room temperature.^{1,2,5,6} From this stock solution, standards of 0, 8, 40, 100, 200, 400, and 600 μM were prepared via dilution with DI water. The amperometric H₂ sensor tip was immersed in each standard, and 6 measurements of the steady state current were taken after at least 2 minutes to generate a current vs. H₂ concentration calibration curve (Figure S3). After calibrating the amperometric H₂ sensor, the scale readings of GPR-H₂ and GPR-N₂ flow tubes were set to desired levels to form a H₂/N₂ gas mixture with defined volume percentages of H₂ (%V_{H₂}) and N₂ (%V_{N₂}). The H₂ concentration of a H₂/N₂ gas mixture was measured using the apparatus in Figure S4. Two mL of DI water was placed in a 1 cm × 1 cm glass vessel and clamped to a support stand. A needle connected to the gas flow apparatus was inserted into the water. H₂/N₂ gas was delivered into the water for 20 minutes by setting the single flow tube rotameter scale reading to 15.00 mm to saturate the solution. The gas flow to the sample was cut off and the H₂ concentration, in μM, was measured by inserting the calibrated amperometric H₂ sensor into the sample and covering the glass vessel with a Teflon cap that had the corner sectioned off. The volume percentage of H₂ (%V_{H₂}) in the H₂/N₂ mixture was calculated according to Equation S4 where [*H₂*]_{measured} was the electrochemically measured μM concentration of H₂ in the H₂/N₂ mixture, and [*H₂*]_{saturated} was the saturated concentration of H₂ in water, which is 800 μM at room temperature and standard pressure.^{1,6,13} The volume percentage of N₂ (%V_{N₂}) in the H₂/N₂ mixture was calculated according to Equation S5. Next, the theoretical density of the H₂/N₂ mixture (*ρ_{mix}*) was calculated via Equation S6 where *MW_{H₂}* and *MW_{N₂}* are the molecular weights of H₂ and N₂, respectively. Once *ρ_{mix}* was known, this value was plugged into Equation S7 to calculate the flow rate of the H₂/N₂ mixture (*Q_{mix}*) at a particular flow tube rotameter scale reading using the calibrated flow of N₂ (*Q_{N₂}*) from Table S2. Three different H₂/N₂ mixtures were made according to the

data shown in Table S3. From the data in Table S3, the flow rates of these sample gases were calculated using Equation S7 at various single flow tube rotameter scale readings, and the results are summarized in Table S4. Plots of flow rate vs. scale reading were made for each gas listed in Table S4, and the results are shown in Figure S5. Quadratic functions were fit to the data in Figure S5 and were then used to calculate the necessary single flow tube rotameter scale reading to deliver sample gas at a 23.40 mL/min flow rate during an experiment. This flow rate was used for all experiments described herein.

Testing Various Indicator/Au-Pd NP Systems for Visual Color Change Upon Reaction with H₂. Aqueous solutions of bromothymol blue, methyl red, and resazurin indicators were prepared in volumetric flasks in 1X PBS buffer, had an indicator concentration of 20 μ M, and had Au-Pd NPs present at 0.8% (v/v). The samples were then exposed to 800 μ M H₂ using the apparatus shown in Figure S6 as UV-Vis absorption spectra of all samples were collected over time.

Resazurin/Au-Pd NP System: Effects of the Concentrations of H₂, Au-Pd NPs, and Resazurin on the Color Change Response Time. The effects of the concentrations of H₂, Au-Pd NPs, and resazurin on the response time of observed color changes within Resazurin/Au-Pd NP systems were studied using the apparatus in Figure S6. In all experiments, 1X PBS buffer was used as the solvent. To study H₂ concentration effects, three identical samples were prepared and had 20 μ M resazurin concentrations and Au-Pd NPs present at 0.8% (v/v). These samples were then exposed to H₂ at 800, 558, and 169 μ M concentrations. The effects of Au-Pd NP concentration were studied by preparing two samples with resazurin concentrations of 20 μ M. Each sample differed in the v/v percentage of Au-Pd NPs present in solution, and the amounts used were 2% and 0.8%. Each sample was then exposed to 800 μ M H₂. The effects of resazurin concentration were studied by preparing three samples with Au-Pd NPs at 0.8% (v/v), varying the resazurin concentrations at 5, 20, and 40 μ M, then exposing each sample to 800 μ M H₂.

Resazurin/Au-Pd NP System: Control Experiments. To elucidate the cause of observed color changes in the Resazurin/Au-Pd NP system, a series of control experiments were performed by flowing pure H₂ or N₂ gases into various sample combinations (Table S5) using the apparatus described in Figure S6. To ensure the UV-Vis absorption signal remained stable during the data collection interval, a sample of Resazurin/Au-Pd NPs was placed in a cuvette and monitored without any gas flow (Experiment 1, Table S5). Gold colloidal nanoparticles (Au NPs) of \sim 25 nm size were synthesized as described previously⁴² to examine if Au had any catalytic effect on the reduction of resazurin by H₂. A master solution of Au NPs was prepared in a similar fashion as described for the Au-Pd NP master solution, except the centrifugation conditions were 7,000 rpm for 10 minutes. A series of controls using N₂ (Experiments 2–7) and H₂ (Experiments 8–12) were then conducted (Table S5). Samples containing resazurin had 20 μ M concentrations. Samples containing NPs had at 0.8% (v/v) concentrations.

RESULTS AND DISCUSSION

Characterization of Au-Pd and Au NPs. UV-Vis, TEM, and DLS instrumentation were used to characterize the Au-Pd and Au NPs (Figure S7). UV-Vis spectra of the as-synthesized

NP solutions of Au-Pd and Au exhibited bands at \sim 520 and \sim 525 nm, respectively (Figure S7A). These bands were attributed to the localized surface plasmon resonance of the Au material within the nanostructures.⁴³ NPs are known to aggregate in high salt concentrations,⁴⁴ and this phenomenon can be seen when samples at 0.8% v/v concentrations were dispersed in buffer (Figure S7A, dashed lines). The average hydrodynamic diameters (\bar{d}) of the Au-Pd and Au NPs were 18.4 and 24.9 nm, respectively (Figure S7D and S7E).

Comparisons of the Visual Color Changes of Various Indicator/Au-Pd NP Systems Upon Reaction with H₂. All indicator/Au-Pd NP systems underwent irreversible and visual color changes upon reaction with H₂ (Figure 2A–C). One reaction pathway involving a blue to yellow color transition was observed for the Bromothymol Blue/Au-Pd NP system upon H₂ exposure for 20 minutes (inset photographs in Figure 2A). UV-Vis absorption spectra of this sample before (navy blue-trace) and 20 minutes after (yellow-trace) H₂ exposure revealed maxima at \sim 615 and \sim 437 nm, respectively (Figure 2A). These values agree nicely with those reported in literature for the protonated and deprotonated forms of pure bromothymol blue.²⁹ However, the observed color changes in Figure 2A are attributed to a redox reaction rather than an acid/base reaction since the solution pH was maintained at neutral throughout the experiment.

For the Methyl Red/Au-Pd NP system, three colors were observed (inset photographs of Figure 2B) and had reaction pathways that proceeded from yellow to colorless during 2 minutes of H₂ exposure, then colorless to faint red after exposure to ambient air for 10 minutes. Similarly, the yellow to colorless transition of the Methyl Red/Au-Pd NP system upon reaction with H₂ is attributed to a redox reaction rather than an acid/base reaction since the solution pH did not change throughout H₂ exposure. UV-Vis absorption spectra of the various sample colors observed for the Methyl Red/Au-Pd NP system before (brownish yellow-trace), and 2 minutes after (black-trace) H₂ exposure revealed maxima at \sim 430 and \sim 305 nm, respectively, while the sample after 10 minutes of air exposure had maxima at \sim 316 nm with additional bands at \sim 514, \sim 552, and \sim 700 nm (Figure 2B).

The Resazurin/Au-Pd NP system also displayed visual color changes upon reaction with H₂, and these data are displayed in Figure 2C. Three colors were observed during the experiment (inset photographs of Figure 2C) and included reaction pathways that went from blue to pink after 1 minute of H₂ exposure, then pink to colorless after additional H₂ exposure for 2 minutes, then colorless to pink after exposure to ambient air. These color changes were attributed to the redox reaction described in Figure 3, in which resazurin (blue color) underwent an irreversible reduction in the presence of H₂ and Au-Pd NP catalysts to form resorufin (pink color) with a subsequent reduction to dihydroresorufin (colorless) that was reversible in the presence of ambient O₂.^{34–36,38} These observations were supported by the spectral data in Figure 2C. For example, the UV-Vis absorption maxima for the Resazurin/Au-Pd NP sample before (blue-trace), and after (pink-trace) H₂ exposure were \sim 601 and \sim 571 nm, respectively (Figure 2C). These maxima agree nicely with those reported in the literature for pure resazurin and resorufin at comparable pH.³⁷ The redox reaction reversibility of dihydroresorufin back to resorufin in the presence of ambient O₂ is well known³⁵ and can be seen

visually in the third photograph in the inset of Figure 2C. This photograph was taken after converting the sample to the colorless form via H₂ exposure, then exposing it to ambient air

for ~2 minutes. A small layer of pink color, corresponding to resorufin, formed at the solution/air interface shortly after exposure to ambient air

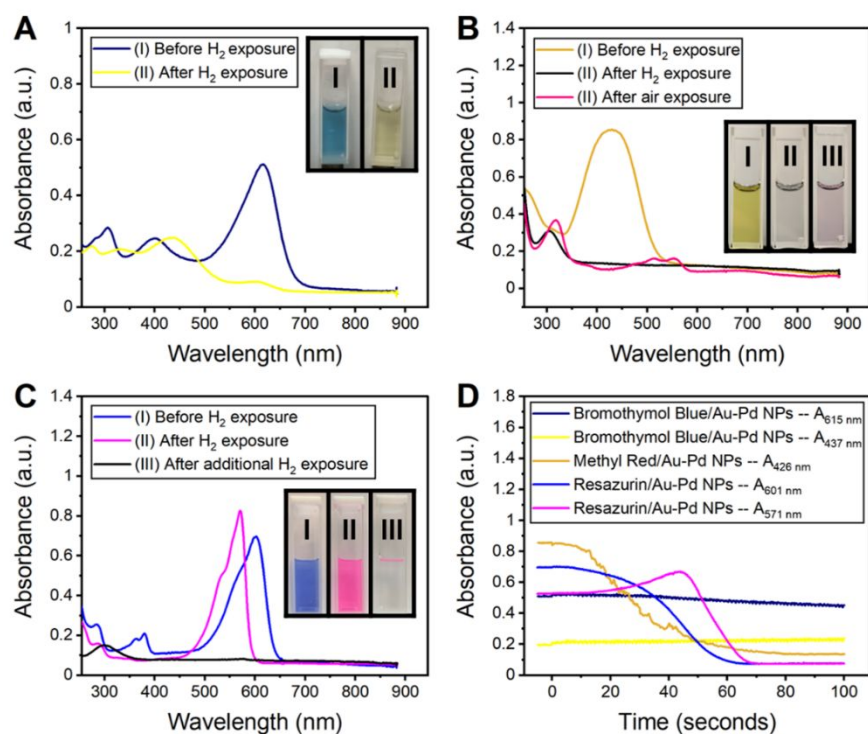


Figure 2. Comparison of the color changes observed for various indicator/Au-Pd NP systems upon reaction with 800 μM H₂. Raw UV-Vis spectra are shown in (A), (B), and (C). The Bromothymol Blue/Au-Pd NP system before (A, navy blue-trace) and after 20 minutes of H₂ exposure (A, yellow-trace). The Methyl Red/Au-Pd NP system before (B, brownish yellow-trace) and after 2 minutes of H₂ exposure (B, black-trace) followed by exposure to air for 10 minutes (B, red-trace). The Resazurin/Au-Pd NP system before (C, blue-trace) and 1 minute after exposure to H₂ (C, pink-trace), and after additional H₂ exposure for 2 minutes (C, black-trace). Inset photographs in (A), (B), and (C) are the sample solution colors observed during the experiment. (D) Comparison of the real-time changes in the characteristic UV-Vis absorption bands for each indicator/Au-Pd NP system as a function of H₂ exposure time.

demonstrating that dihydroresorufin is very sensitive to O₂. The colorless solution eventually reverted back to a full pink color after ~30 minutes of air exposure. Like the other indicator/Au-Pd NP systems investigated, the pH of the Resazurin/Au-Pd NP system did not change throughout experimentation with H₂.

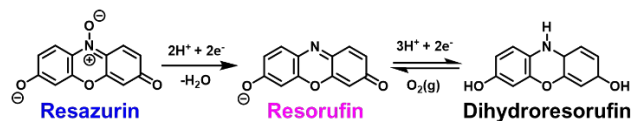


Figure 3. Redox reactions of resazurin upon reaction with H₂ in the presence of Au-Pd NP catalysts at pH ~7.5.

The characteristic UV-Vis absorption maxima of all indicator/Au-Pd NP samples as a function of H₂ exposure time are displayed in Figure 2D. It is evident from these data that the Bromothymol Blue/Au-Pd NP system had a much slower color change response to H₂ compared to the other systems investigated since the disappearance of the blue color and formation of the yellow color (navy-blue and yellow traces in Figure 2D, respectively) did not change significantly after 100

seconds of H₂ exposure. These results suggest that much longer exposure times would be required to induce a detectable color change. Therefore, bromothymol blue would not be a practical indicator for future H₂ sensor development for our target application. The Methyl Red/Au-Pd NP system had relatively fast color change response to H₂ since the UV-Vis absorption maxima corresponding to the yellow form of methyl red (brownish-yellow trace in Figure 2D) decreased quickly during H₂ exposure. With respect to redox reactions, researchers have shown that methyl red can electrochemically undergo an irreversible reduction to form anthranilic acid and N,N-dimethyl-p-phenylenediamine as products,^{32,33} of which the latter product is known to exhibit acute toxicity.⁴⁵ Consequently, methyl red was not used as an indicator for our research objectives in order to avoid toxic chemicals that would be problematic for medical applications. The Resazurin/Au-Pd NP system also displayed fast color change response to H₂ since the resazurin band (blue-trace in Figure 2D) sharply declined while the resorufin band (pink-trace in Figure 2D) increased to a maximum and eventually flatlined as H₂ was further introduced into the system and all molecules were converted to dihydroresorufin.

Of the three systems we examined, the Resazurin/Au-Pd NP system was best suited for our research objective of future optical H₂ sensor development because (1) this system had fast color change response to H₂ compared to the other indicator/NP systems tested, (2) resazurin has well-studied reduction pathways that involve an initial irreversible reduction to a highly luminescent resorufin product, and (3) the reactants and products involved in the overall redox processes are non-toxic and appropriate for medical applications. For these reasons, the effects of the concentrations of H₂, Au-Pd NPs, and resazurin on the response time of observed color changes within the Resazurin/Au-Pd NP system were studied.

Resazurin/Au-Pd NP System: Effects of the Concentrations of H₂, Au-Pd NPs, and Resazurin on the Color Change Response Time. The effects of H₂ are shown in the time-based UV-Vis absorption spectra of Resazurin/Au-Pd NP systems exposed to H₂ at 169, 558, and 800 μM concentrations (Figure 4A). These data illustrate how decreasing the H₂ concentration exposed to a Resazurin/Au-Pd NP system decreased the color change response time. For example, when monitoring the resazurin bands over time (dashed-line traces in Figure 4A), these bands flatlined after ~65, 125, and 1000 seconds of H₂ exposure for the experiments at 800, 558, and 169 μM H₂ concentrations, respectively. Similarly, the peaks corresponding to resorufin (solid-line traces in Figure 4A) reached maxima after ~50, 100, and 800 seconds of H₂ exposure for the experiments at 800, 558, and 169 μM H₂ concentrations, respectively.

The effects of the concentration of Au-Pd NPs on the Resazurin/Au-Pd NP system are shown in Figure 4B. Comparing the resazurin bands (dashed-line traces in Figure 4B), the sample containing 2% (v/v) Au-Pd NPs flatlined at ~70 seconds while the sample containing 0.8% (v/v) Au-Pd NPs flatlined at ~90 seconds. Comparing the resorufin bands (solid-line traces in Figure 4B), the sample containing a larger amount of Au-Pd NPs reached a maximum at ~54 seconds while the sample containing a lower amount of Au-Pd NPs reached a maximum at ~58 seconds. These data show how increasing the concentration of Au-Pd NPs within the Resazurin/Au-Pd NP system decreased the color change response time upon reaction with H₂.

The effects of the concentration of resazurin on the Resazurin/Au-Pd NP system are shown in Figure 4C. It is evident from these data that the sample containing the lower concentration of resazurin (blue traces in Figure 4C) underwent a faster color change since the resazurin band (blue dashed-line trace in Figure 4C) flatlined much earlier compared to other samples and the resorufin band (blue solid-line trace in Figure 4C) reached a maximum earlier than the other samples. The data obtained in this section demonstrate that the Resazurin/Au-Pd NP system is viable for the future development of optical H₂ sensors for our target application because the system quickly changed color upon reaction with H₂ at levels relevant to *in vivo* Mg-implant biodegradation on a practical time scale, and the H₂ sensing elements can be optimized to achieve a faster or

slower color change response to H₂ by varying the relative amounts of resazurin and Au-Pd NPs.

Resazurin/Au-Pd NP System: Control Experiments. From the set of control experiments described in Table S5, it was observed that the UV-Vis absorption bands in Experiment 1 were very stable and remained nearly constant across the visible wavelength range during measurement with no gas flow (Figure S8). Similar results were observed in Experiments 2–7 as N₂ was delivered into solutions (Figure S9). By comparison, flowing H₂ in Experiments 8–11 gave the same lack of spectral change until both resazurin and AuNPs were present as shown in Figure S10. These observations confirm that N₂ had no effect on the observed color changes for the Resazurin/Au-Pd NP system and that color changes only arose when H₂ reacted with resazurin in the presence of Au-Pd and Au NP catalysts. For example, exposure of H₂ in Experiment 12 (Table S5) to the sample containing resazurin and Au NPs led to dramatic UV-Vis spectral changes as the peaks corresponding to resazurin and resorufin increased and decreased, respectively (Figures S10E and S11). These results show that the Au NPs catalyzed the reduction of resazurin by H₂ to form resorufin, and it has been shown in the literature that Au can catalyze the dissociation of molecular H₂ into hydrogen atoms.^{46,47} Comparing the color change response times of the Resazurin/Au NP (Figure S11) and the Resazurin/Au-Pd NP systems (Figure 2D), the system containing Au-Pd NPs underwent faster color changes. This result was attributed to the presence of Pd in the nanostructures. Pd NPs have been shown to be more effective catalysts for H₂ sensing than those of Au.⁴⁸ Also, Au-Pd alloys have been shown to exhibit accelerated H₂ adsorption compared to Pd.²⁶ The Resazurin/Au NP sample could not be converted to the colorless form, even after 10 minutes of H₂ exposure (data not shown) while the Resazurin/Au-Pd NP system was fully converted to the colorless form after ~65 seconds of H₂ exposure (Figure 2D). These results highlight the importance of Pd on the overall color change response time of the Resazurin/Au-Pd system upon reaction with H₂.

CONCLUSIONS

We have studied various indicator/Au-Pd NP systems that are potentially useful for a variety of optical H₂ sensing applications since each system underwent visible and irreversible color changes upon reaction with H₂ in the presence of Au-Pd NP catalysts in solution. The indicators studied were bromothymol blue, methyl red, and resazurin, and the reactions of each system with H₂ in presence of Au-Pd NPs were concluded to proceed via redox processes. The Resazurin/Au-Pd NP system was deemed best suited for our target application of future optical H₂ sensor development for non-invasive monitoring of *in vivo* Mg-implant biodegradation in medical research and clinical settings because (1) this system had a fast color change response to H₂ compared to the other indicator/Au-Pd NP systems tested, (2) resazurin has well-studied reduction pathways that involve

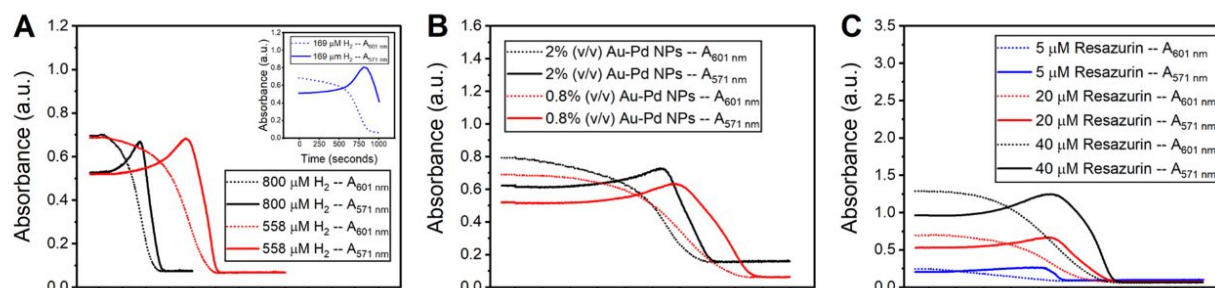


Figure 4. Effects of the concentrations of (A) H₂, (B) Au-Pd NPs, and (C) resazurin on the color change response time of the Resazurin/Au-Pd NP system. The bands corresponding to Resazurin (dashed lines) and resorufin (solid lines) were monitored over time during H₂ exposure.

an initial irreversible reduction to a highly luminescent resorufin product, and (3) the reactants and products involved in the overall redox processes are non-toxic and appropriate for medical applications. Studying the effects of the concentrations of H₂, Au-Pd NPs, and resazurin on the color change response time within the Resazurin/Au-Pd NP system revealed that the sensing elements can be optimized to achieve a faster or slower color change with H₂ by varying the relative amounts of resazurin and Au-Pd NPs.

The other indicator/Au-Pd NP systems were deemed unsuitable and impractical for our research objectives because the system involving bromothymol blue exhibited a relatively slow color change upon exposure to H₂, and the system involving methyl red presumably formed a redox product with acute toxicity (i.e. N,N-dimethyl-p-phenylenediamine). Both the color change response time and the H₂ concentration range tested for the Resazurin/Au-Pd NP system are appropriate for our intended application of monitoring the biodegradation of Mg-implants used for bone repair and other medical procedures.

Although this research was driven by our interest in developing better H₂ sensors for non-invasive monitoring of *in vivo* biodegradation of Mg-based implants, the materials explored here are potentially useful for other H₂ sensing applications such as leak detection wherever H₂ is used.

ASSOCIATED CONTENT

Supporting Information

The Supporting Information is available free of charge on the ACS Publications website.

Figures, tables, and equations describing various gas flow setups and determinations of flow rates of N₂, H₂, and H₂/N₂ gases; TEM characterizations of Au-Pd and Au NPs; and UV-Vis spectra of control experiments (PDF).

AUTHOR INFORMATION

Corresponding Author

* Email: zhangph@ucmail.uc.edu. Phone: 513/556-9222.

* Email: heinemwr@ucmail.uc.edu. Phone: 513/556-9210.

ORCID

Michael E. Smith: 0000-0002-4295-8917

Peng Zhang: 0000-0003-3902-6876

William R. Heineman: 0000-0003-2428-5445

Author Contributions

M.E.S, W.R.H., and P.Z. designed the research project. M.E.S. wrote the manuscript, and designed/carried out all experiments and measurements, except for TEM measurements. A.L.S. critically revised the manuscript and provided a program to analyze UV-Vis spectra. Z.Y. acquired TEM images of nanoparticle samples. J.A.L. provided technical assistance with the amperometric H₂ sensor.

Notes

The authors declare no competing financial interest.

ACKNOWLEDGMENT

The authors gratefully acknowledge the National Science Foundation for financial support (NSF ERC 0812348). Dr. Patrick Slonecker is acknowledged for his assistance with gas flow setups.

REFERENCES

- (1) Kuhlmann, J.; Witte, F.; Heineman, W. R. Electrochemical Sensing of Dissolved Hydrogen in Aqueous Solutions as a Tool to Monitor Magnesium Alloy Corrosion. *Electroanalysis* **2013**, *25* (5), 1105–1110.
- (2) Kuhlmann, J.; Bartsch, I.; Willbold, E.; Schuchardt, S.; Holz, O.; Hort, N.; Höche, D.; Heineman, W. R.; Witte, F. Fast Escape of Hydrogen from Gas Cavities around Corroding Magnesium Implants. *Acta Biomater.* **2013**, *9* (10), 8714–8721.
- (3) Han, H. S.; Loffredo, S.; Indong, J.; Edwards, J.; Kim, Y. C.; Seok, H. K.; Witte, F.; Mantovani, D.; Glyn-Jones, S. Current Status and Outlook on the Clinical Translation of Biodegradable Metals. *Mater. Today* **2019**, *23*, 57–71.
- (4) Zhao, D.; Wang, T.; Guo, X.; Kuhlmann, J.; Doepke, A.; Dong, Z.; Shanov, V. N.; Heineman, W. R. Monitoring Biodegradation of Magnesium Implants with Sensors. *Jom* **2016**, *68* (4), 1204–1208.
- (5) Zhao, D.; Wang, T.; Hoagland, W.; Benson, D.; Dong, Z.; Chen, S.; Chou, D. T.; Hong, D.; Wu, J.; Kumta, P. N.; et al. Visual H₂ Sensor for Monitoring Biodegradation of Magnesium Implants in Vivo. *Acta Biomater.* **2016**, *45*, 399–409.
- (6) Zhao, D.; Wang, T.; Kuhlmann, J.; Dong, Z.; Chen, S.; Joshi, M.; Salunke, P.; Shanov, V. N.; Hong, D.; Kumta, P. N.; et al. In Vivo Monitoring the Biodegradation of Magnesium Alloys with an Electrochemical H₂ Sensor. *Acta Biomater.* **2016**, *36*, 361–368.
- (7) Witte, F.; Kaese, V.; Haferkamp, H.; Switzer, E.; Meyer-Lindenberg, A.; Wirth, C. J.; Windhagen, H. In Vivo Corrosion of Four Magnesium Alloys and the Associated Bone Response. *Biomaterials* **2005**, 3557–3563.
- (8) Witte, F.; Calliess, T.; Windhagen, H. Biodegradable Synthetic Implant Materials: Clinical Applications and Immunological Aspects. *Orthopade* **2008**, *37* (2), 125–130.
- (9) Banerjee, P. C.; Al-Saadi, S.; Choudhary, L.; Harandi, S. E.; Singh, R. Magnesium Implants: Prospects and Challenges. *Materials (Basel)*. **2019**, *12* (1), 1–21.
- (10) Song, G. Control of Biodegradation of Biocompatible Magnesium Alloys. *Corros. Sci.* **2007**, *49* (4), 1696–1701.
- (11) Weber, M. J.; Kim, J. H.; Lee, J. H.; Kim, J. Y.; Iatsunskyi, I.; Coy, E.; Drobek, M.; Julbe, A.; Bechelany, M.; Kim, S. S.; et al. High Performance Nanowires Hydrogen Sensors by Exploiting the Synergistic Effect of Pd Nanoparticles and MOF Membranes. *ACS Appl. Mater. Interfaces* **2018**, *10* (40), 34765–34773.
- (12) Zhao, D.; Wu, J.; Chou, D.; Hoagland, W.; Benson, D.; Dong, Z.; Kumta, P. N.; Heineman, W. R. Visual Hydrogen Mapping Sensor for Noninvasive Monitoring of Bioresorbable Magnesium Implants In Vivo. *JOM* **2020**, *72* (5), 1851–1858.
- (13) Seo, T.; Kurokawa, R.; Sato, B. A Convenient Method for Determining the Concentration of Hydrogen in Water: Use of Methylene Blue with Colloidal Platinum. *Med. Gas Res.* **2012**, *2* (1), 1–6.
- (14) Chen, J.; Zhang, J.; Wang, M.; Li, Y. High-Temperature Hydrogen Sensor Based on Platinum Nanoparticle-Decorated SiC Nanowire Device. *Sensors Actuators, B Chem.* **2014**, *201*, 402–406.
- (15) Hussain, G.; Ge, M.; Zhao, C.; Silvester, D. S. Fast Responding Hydrogen Gas Sensors Using Platinum Nanoparticle Modified Microchannels and Ionic Liquids. *Anal. Chim. Acta* **2019**, *1072*, 35–45.
- (16) Jung, D.; Han, M.; Lee, G. S. Fast-Response Room Temperature Hydrogen Gas Sensors Using Platinum-Coated Spin-Capable Carbon Nanotubes. *ACS Appl. Mater. Interfaces* **2015**, *7* (5), 3050–3057.
- (17) Paquin, F.; Rivnay, J.; Salleo, A.; Stingelin, N.; Silva, C. Multi-Phase Semicrystalline Microstructures Drive Exciton Dissociation in Neat Plastic Semiconductors. *J. Mater. Chem. C* **2015**, *3*, 10715–10722.
- (18) Kalanur, S. S.; Lee, Y.; Seo, H. Eye-Readable Gasochromic and Optical Hydrogen Gas Sensor Based on CuS-Pd. *RSC Adv.* **2015**, *5*, 9028–9034.
- (19) Sterl, F.; Strohhfeldt, N.; Herkert, E.; Weiss, T.; Giessen, H. Design Principles for Sensitivity Optimization in Plasmonic Hydrogen Sensors. *ACS Sensors* **2020**, A-K.

- (20) Subramanian, S.; Kumar, K.; Dhawan, A. Palladium-Coated Narrow Groove Plasmonic Nanogratings for Highly Sensitive Hydrogen Sensing. *RSC Adv.* **2020**, *10* (7), 4137–4147.
- (21) Chiu, C.; Huang, M. H. Polyhedral Au – Pd Core – Shell Nanocrystals as Highly Spectrally Responsive and Reusable Hydrogen Sensors in Aqueous Solution. *Angew. Chemie - Int. Ed.* **2013**, *52*, 12709–12713.
- (22) Jiang, R.; Qin, F.; Ruan, Q.; Wang, J.; Jin, C. Ultrasensitive Plasmonic Response of Bimetallic Au / Pd Nanostructures to Hydrogen. *Adv. Funct. Mater.* **2014**, *24*, 7328–7337.
- (23) Nasir, M. E.; Dickson, W.; Wurtz, G. A.; Wardley, W. P.; Zayats, A. V. Hydrogen Detected by the Naked Eye : Optical Hydrogen Gas Sensors Based on Core / Shell Plasmonic Nanorod Metamaterials. *Adv. Mater.* **2014**, *26*, 3532–3537.
- (24) Rajoua, K.; Baklouti, L.; Favier, F. Electronic and Mechanical Antagonist Effects in Resistive Hydrogen Sensors Based on Pd@Au Core–Shell Nanoparticle Assemblies Prepared by Langmuir–Blodgett. *J. Phys. Chem. C* **2015**, *119*, 10130–10139.
- (25) Yip, H. K.; Zhu, X.; Zhuo, X.; Jiang, R.; Yang, Z.; Wang, J. Gold Nanopyramid-Enhanced Hydrogen Sensing with Plasmon Red Shifts Reaching ≈ 140 nm at 2 Vol % Hydrogen Concentration. *Adv. Opt. Mater.* **2017**, *5*, 1700740–1700753.
- (26) Namba, K.; Ogura, S.; Ohno, S.; Di, W.; Kato, K.; Wilde, M.; Pletikoscic, I.; Pervan, P.; Milun, M.; Fukutani, K. Acceleration of Hydrogen Absorption by Palladium through Surface Alloying with Gold. *Proc. Natl. Acad. Sci. U. S. A.* **2018**, *115* (31), 7896–7900.
- (27) Wadell, C.; Nugroho, F. A. A.; Lidström, E.; Iandolo, B.; Wagner, J. B.; Langhammer, C. Hysteresis-Free Nanoplasmonic Pd–Au Alloy Hydrogen Sensors. *Nano Lett.* **2015**, *15* (5), 3563–3570.
- (28) Galagan, Y.; Su, W. F. Reversible Photoreduction of Methylene Blue in Acrylate Media Containing Benzyl Dimethyl Ketal. *J. Photochem. Photobiol. A Chem.* **2008**, *195*, 378–383.
- (29) Shimada, T.; Hasegawa, T. Determination of Equilibrium Structures of Bromothymol Blue Revealed by Using Quantum Chemistry with an Aid of Multivariate Analysis of Electronic Absorption Spectra. *Spectrochim. Acta - Part A Mol. Biomol. Spectrosc.* **2017**, *185*, 104–110.
- (30) Harris, D. C. *Quantitative Chemical Analysis*, 7th ed.; W. H. Freeman and Co.: New York, NY, 2007.
- (31) Chandrashekar, B. N.; Swamy, B. E. K.; Mahesh, K. R. V.; Chandra, U.; Sherigara, B. S. Electrochemical Studies of Bromothymol Blue at Surfactant Modified Carbon Paste Electrode by Using Cyclic Voltammetry. *Int. J. Electrochem. Sci.* **2009**, *4*, 471–480.
- (32) Umeno, M.; Yanagita, K.; Sagami, I.; Shimizu, T. Azo Reduction Catalyzed by Cytochrome P450 1A2 and NADPH-Cytochrome P450 Reductase. *Environ. Bioinorg. Chem.* **1997**, *67*, 379.
- (33) Xu, G.; O'Dea, J. J.; Osteryoung, J. G. Surface Reduction Study of Monoazo Dyes by Adsorptive Square Wave Voltammetry. *Dye. Pigment.* **1996**, *30* (3), 201–223.
- (34) Khazalpour, S.; Nematollahi, D. Electrochemical Study of Alamar Blue (Resazurin) in Aqueous Solutions and Room-Temperature Ionic Liquid 1-Butyl-3-Methylimidazolium Tetrafluoroborate at a Glassy Carbon Electrode. *RSC Adv.* **2014**, *4* (17), 8431–8438.
- (35) Mills, A.; Wang, J.; McGrady, M. Method of Rapid Assessment of Photocatalytic Activities of Self-Cleaning Films. *J. Phys. Chem. B* **2006**, *110* (37), 18324–18331.
- (36) Oja, S. M.; Guerrette, J. P.; David, M. R.; Zhang, B. Fluorescence-Enabled Electrochemical Microscopy with Dihydroresorufin as a Fluorogenic Indicator. *Anal. Chem.* **2014**, *86* (12), 6040–6048.
- (37) Porcal, G. V.; Altamirano, M. S.; Glusko, C. A.; Bertolotti, S. G.; Previtali, C. M. Photophysical Properties of the Phenoxazin Dyes Resazurin and Resorufin in Soybean Lecithin Microemulsions. *Dye. Pigment.* **2011**, *88* (3), 240–246.
- (38) Tratnyek, P. G.; Reilkoff, T. E.; Lemon, A. W.; Scherer, M. M.; Balko, B. A.; Feik, L. M.; Henegar, B. D. Visualizing Redox Chemistry: Probing Environmental Oxidation-Reduction Reactions with Indicator Dyes. *Chem. Educ.* **2001**, *6*, 172–179.
- (39) Liu, X.; Chen, T.; Song, P.; Zhang, Y.; Xu, W. Single-Molecule Nanocatalysis of Pt Nanoparticles. *J. Phys. Chem. C* **2018**, *122* (3), 1746–1752.
- (40) Han, J.; Zhou, Z.; Yin, Y.; Luo, X.; Li, J.; Zhang, H.; Yang, B. One-Pot, Seedless Synthesis of Flowerlike Au-Pd Bimetallic Nanoparticles with Core-Shell-like Structure via Sodium Citrate Coreduction of Metal Ions. *CrystEngComm* **2012**, *14* (20), 7036–7042.
- (41) Caplan, K. J. Rotameter Corrections for Gas Density. *Am. Ind. Hyg. Assoc. J.* **1985**, *46* (11), B10–B16.
- (42) Yu, Z.; Smith, M. E.; Zhang, J.; Zhou, Y.; Zhang, P. Determination of Trichloroethylene by Using Self-Referenced SERS and Gold-Core/Silver-Shell Nanoparticles. *Microchim. Acta* **2018**, *185* (7), 2–8.
- (43) Willets, K. A.; Van Duyne, R. P. Localized Surface Plasmon Resonance Spectroscopy and Sensing. *Annu. Rev. Phys. Chem.* **2007**, *58* (19), 267–297.
- (44) Christau, S.; Moeller, T.; Genzer, J.; Koehler, R.; Von Klitzing, R. Salt-Induced Aggregation of Negatively Charged Gold Nanoparticles Confined in a Polymer Brush Matrix. *Macromolecules* **2017**, *50* (18), 7333–7343.
- (45) Safety Data Sheet for N,N-Dimethyl-p-phenylenediamine <https://www.sigmaaldrich.com/MSDS/MSDS/DisplayMSDSPage.do?country=US&language=en&productNumber=193992&brand=ALDRICH&PageToGoToURL=https%3A%2F%2Fwww.sigmaaldrich.com%2Fcatalog%2Fproduct%2Faldrich%2F193992%3Fflang%3Den> (accessed Jan 7, 2020).
- (46) Tran, T. D.; Nguyen, M. T. T.; Le, H. V.; Nguyen, D. N.; Truong, Q. D.; Tran, P. D. Gold Nanoparticles as an Outstanding Catalyst for the Hydrogen Evolution Reaction. *Chem. Commun.* **2018**, *54* (27), 3363–3366.
- (47) Gatin, A.; Grishin, M.; Dokhlikova, N.; Ozerin, S.; Sarvadii, S.; Kharitonov, V.; Shub, B. Effect of Size on Hydrogen Adsorption on the Surface of Deposited Gold Nanoparticles. *Nanomaterials* **2019**, *9* (3), 1–8.
- (48) Shim, Y.; Zhang, L.; Kim, D. H.; Kim, Y. H.; Choi, Y. R.; Nahm, S. H.; Kang, C.; Lee, W.; Jang, H. W. Highly Sensitive and Selective H₂ and NO₂ Gas Sensors Based on Surface-Decorated WO₃ Nanoigloos. *Sensors Actuators B. Chem.* **2014**, *198*, 294–301.

FOR TABLE OF CONTENTS ONLY

